Pergamon

Solid State Communications, Vol. 104, No. 7, pp. 401–405, 1997

0038–1098/97 $17.00+.00

PII: S0038–1098(97)00339-6

ELECTRONIC TRANSITIONS IN InAs NANOCRYSTALS USING WANNIER FUNCTION METHOD

Ari Mizel and Marvin L. Cohen

Department of Physics, University of California at Berkeley, Berkeley, CA 94720, U.S.A. and
Materials Science Division, Lawrence Berkeley National Laboratory, Berkeley, CA 94720, U.S.A.

(*Received* 3 *July* 1997; *accepted* 14 *July* 1997 *by S.G. Louie*)

A Wannier function method is employed to compute electronic transitions in InAs nanocrystals. Our calculations agree well with experimental results, in contrast to the predictions of multiband $\mathbf{k}\cdot\mathbf{p}$ theory. This success results from our accurate treatment of the bulk band structure. We also predict the energies of higher electronic transitions. © 1997 Elsevier Science Ltd

Semiconductor nanocrystals have generated exciting questions in basic and applied science [1]. Considerable attention has been directed toward the size dependence of nanocrystal electronic structure, especially the size dependence of the fundamental electronic gap [2–12]. Photoabsorption, photoemission and photoluminescence studies have produced increasingly detailed experimental information about electronic spectra [2–4]. The theoretical problem of computing nanocrystal electronic levels is a field of active research [5–12].

In particular, InAs nanocrystals present an interesting case for theorists. Because the dielectric constant of bulk InAs is large, the electron–hole Coulomb energy should be relatively small. This is an advantageous situation since the Coulomb energy can be difficult to compute accurately [13].

In this paper, we utilize our Wannier function method [14] to compute InAs nanocrystal transitions. The calculation begins with a computation of the bulk bands, for which we employ the empirical pseudopotential method (EPM) [15]. Using this EPM band structure, we determine the nanocrystal electronic levels as a function of size. Our results are in good agreement with experimental data [16]. This success must be contrasted with the overpredictions of effective mass theory [6] and current multiband $\mathbf{k}\cdot\mathbf{p}$ theory [5] applied to InAs nanocrystal transitions.

The Wannier function method is described in a previous paper [14]. Here, we outline our procedure and then describe some improvements in our computational implementation.

For a bulk system, the Wannier function $a_n(\mathbf{r}-\mathbf{R})$ is defined in terms of the Bloch functions $\psi_{n,\mathbf{k}}(\mathbf{r})$ by [17]

$$a_n(\mathbf{r}-\mathbf{R}) \equiv \frac{1}{\sqrt{\Omega}}\int_{BZ} \mathrm{d}^3k\, \mathrm{e}^{-i\mathbf{k}\cdot\mathbf{R}}\,\psi_{n,\mathbf{k}}(\mathbf{r}). \tag{1}$$

In this equation, n is a band index, $\mathbf{R}$ is a lattice vector, Ω is the volume of the first Brillouin zone (BZ) and the integral proceeds over the BZ. The Wannier functions provide an orthonormal basis and the function $a_n(\mathbf{r}-\mathbf{R})$ is localized about the site $\mathbf{R}$. These properties suggest the use of Wannier functions as orbitals in a tight-binding type calculation.

We can obtain the interaction matrix elements between two Wannier functions as follows. Using the fact that the Bloch functions are energy eigenstates,

$$H_{bulk}\psi_{n,\mathbf{k}}(\mathbf{r}) = E_n(\mathbf{k})\psi_{n,\mathbf{k}}(\mathbf{r}), \tag{2}$$

it follows from definition (1) that

$$\langle a_{n,\mathbf{R}_i}|H_{bulk}|a_{m,\mathbf{R}_j}\rangle = \int a_n^*(\mathbf{r}-\mathbf{R}_i)H_{bulk}a_m(\mathbf{r}-\mathbf{R}_j)\,\mathrm{d}^3r = \delta_{m,n}\tilde{E}_n(\mathbf{R}_i-\mathbf{R}_j). \tag{3}$$

Here,

$$\tilde{E}_n(\mathbf{R}) \equiv \frac{1}{\Omega}\int_{BZ} \mathrm{d}^3k\, \mathrm{e}^{i\mathbf{k}\cdot\mathbf{R}}\,E_n(\mathbf{k}), \tag{4}$$

is a kind of Fourier component of the bulk band structure. Note that the matrix elements (3) are block diagonal in the band index.

To model the eigenstates of a nanocrystal, we diagonalize the matrix $\langle a_{n,\mathbf{R}_i}|H_{bulk}|a_{n,\mathbf{R}_j}\rangle$ for a given band n, where the $\mathbf{R}_i$ and $\mathbf{R}_j$ are restricted to the nanocrystal interior. This restriction captures the physics of the finite size of the nanocrystal. The procedure is reasonable provided that (1) within the nanocrystal, the Hamiltonian is similar to the Hamiltonian of the bulk and (2) the nanocrystal wavefunctions decay sufficiently rapidly into the vacuum that they can be modelled using only Wannier functions localized inside the nanocrystal interior. The second condition corresponds, within effective mass models, to placing an infinite barrier at the nanocrystal boundaries. It should be noted that at no stage in our calculation do we introduce a fitting parameter corresponding to a finite barrier height. As pointed out by Norris and Bawendi [2], such a fitting parameter typically is not physically meaningful but instead handles general deviations between theory and experiment.

The eigenvalues of the matrix $\langle a_{n,\mathbf{R}_i}|H_{bulk}|a_{n,\mathbf{R}_j}\rangle$ are envelope functions $f_n^\alpha(\mathbf{R})$ satisfying

$$\sum_{\mathbf{R}_i}\langle a_{n,\mathbf{R}_i}|H_{bulk}|a_{n,\mathbf{R}_j}\rangle f_n^\alpha(\mathbf{R}_j) = E_n^\alpha f_n^\alpha(\mathbf{R}_i), \tag{5}$$

where the sum proceeds over unit cells in the nanocrystal interior. For each band, n, the eigenvectors are labelled by an index α that takes values between 1 and the number of cells in the nanocrystal. Once the envelope functions $f_n^\alpha(\mathbf{R})$ have been found, the energy eigenstates of the nanocrystal are assumed to take the form

$$\Psi_n^\alpha(\mathbf{r}) = \sum_{\mathbf{R}} f_n^\alpha(\mathbf{R}) a_n(\mathbf{r}-\mathbf{R}), \tag{6}$$

where the sum proceeds over the unit cells inside the nanocrystal.

To actually implement the procedure outlined above, we first make an EPM calculation of the band structure $E_n(\mathbf{k})$. Our EPM calculation includes nonlocal effects and spin–orbit coupling according to the paper of Chelikowsky and Cohen [18]. However, instead of using perturbation theory to include the spin–orbit interaction as they do, we directly diagonalize the full EPM Hamiltonian $H_{\mathbf{G},s,\mathbf{G},s'}(\mathbf{k})$. We obtain the same band structure, but to do so we set the spin–orbit parameter to the value $\mu = 0.0048$, rather than their value of $\mu = 0.0012$. Once the EPM band structure is calculated, we obtain the matrix elements (3) by numerical integration.

Finally, we are in a position to diagonalize the matrix $\langle a_{n,\mathbf{R}_i}|H_{bulk}|a_{n,\mathbf{R}_j}\rangle$, with $\mathbf{R}_i$ and $\mathbf{R}_j$ restricted to the nanocrystal interior. In this paper, we always restrict these lattice vectors to lie within a sphere to model a nanocrystal with a round arrangement of unit cells. Spherical nanocrystals as large as 70 Å in diameter (3367 unit cells) are considered in this way. The matrix diagonalization yields the desired envelope function eigenvectors f_n^α and eigenenergies E_n^α.

Before giving the results of our calculations, we state selection rules governing dipole transitions between electronic states. The dipole matrix element between the αth state in the mth band and the βth state in the nth band is

$$\begin{aligned}\langle m,\alpha|\mathbf{p}|n,\beta\rangle &\equiv \int d^3r \left[\sum_{\mathbf{R}} f_m^{*\alpha}(\mathbf{R}) a_m^*(\mathbf{r}-\mathbf{R})\right]\mathbf{p} \\ &\quad\times\left[\sum_{\mathbf{R}'} f_n^\beta(\mathbf{R}') a_n(\mathbf{r}-\mathbf{R}')\right] \\ &\approx \left[\sum_{\mathbf{R}} f_m^{*\alpha}(\mathbf{R}) f_n^\beta(\mathbf{R})\right]\int d^3r\, a_m^*(\mathbf{r})\mathbf{p}a_n(\mathbf{r}).\end{aligned} \tag{7}$$

In the last line, we have assumed that the matrix element of $\mathbf{p}$ between Wannier functions localized on different sites is small. The sum over lattice sites only includes positions within the nanocrystal interior. The sum requires that, in allowed transitions, the initial envelope function and the final envelope function have nonzero overlap.

When we examine the results of our computer calculations, it turns out that the HOMO state, denoted $f_v^{(1)}(\mathbf{R})$, turns out to be s-like, as shown in Fig. 1. In the notation $f_v^{(1)}$, the subscript v refers to the highest valence

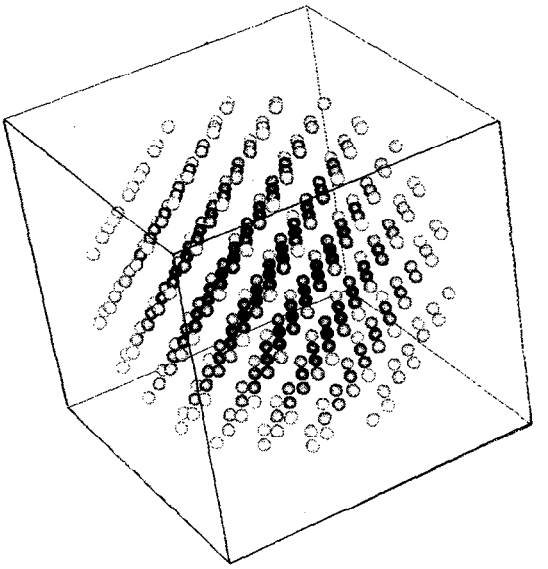

Fig. 1. HOMO state for small nanocrystal. Each sphere represents a unit cell. A dark sphere indicates a large value for envelope function $f_v^{(1)}(\mathbf{R})$ in that unit cell. The figure shows the s-like character of $f_v^{(1)}$.

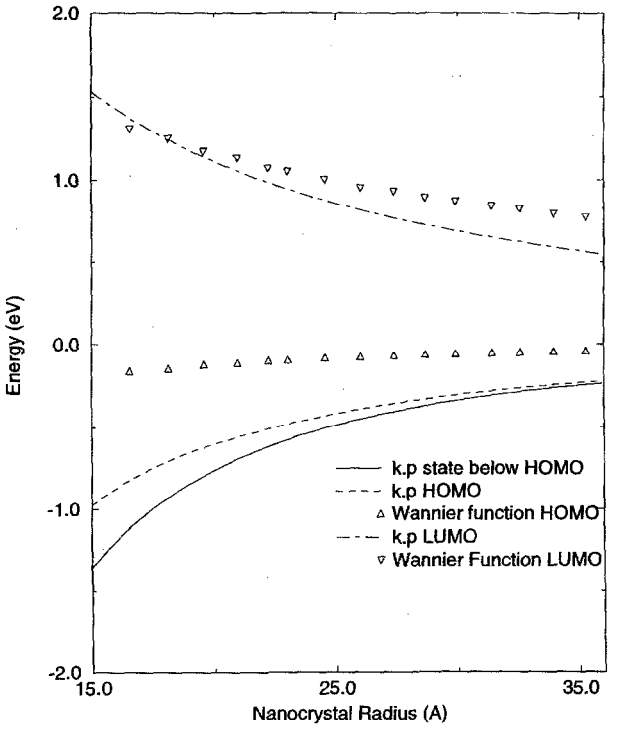

Fig. 2. LUMO and HOMO state energies as a function of nanocrystal radius. Both Wannier function theory and multiband **k·p** theory predict *s*-like LUMO states. Wannier function method predicts an *s*-like HOMO state. Multiband **k·p** theory predicts an odd parity HOMO state, so that the fundamental transition to LUMO occurs from state below HOMO.

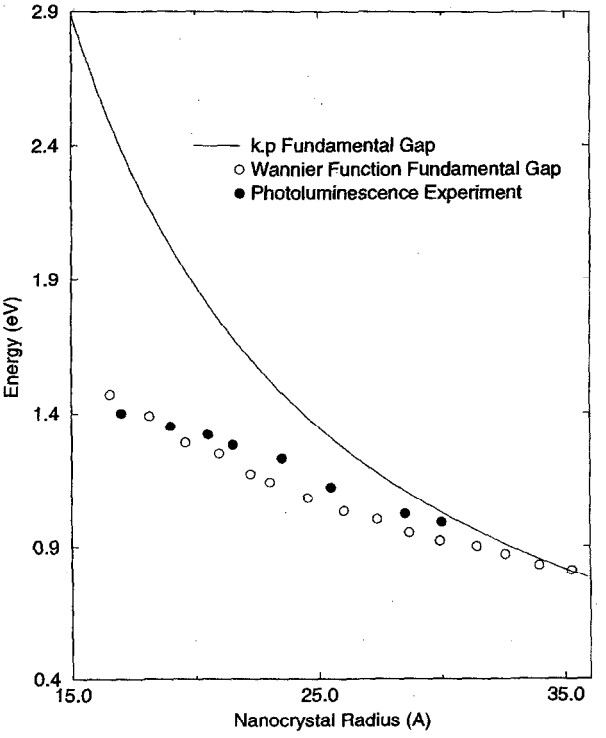

Fig. 3. The energy of the fundamental gap vs nanocrystal radius. The Wannier function prediction is in good agreement with data.

band and the superscript (1) refers to the fact that, of the states derived from that band, the HOMO has energy closest to the bulk valence band maximum. A similar plot for the LUMO state, $f_c^{(1)}(\mathbf{R})$, shows that it is also *s*-like. Therefore, a dipole transition is allowed assuming the Wannier function integral is nonzero.

The energy of our LUMO and HOMO are plotted in Fig. 2 as a function of nanocrystal radius. On the same plot, we show the energy of multiband $\mathbf{k}\cdot\mathbf{p}$ states, calculated using the formalism of reference [5]. The InAs band parameters required for the multiband $\mathbf{k}\cdot\mathbf{p}$ calculation were taken from the literature [19]. The Wannier function method and the multiband $\mathbf{k}\cdot\mathbf{p}$ theory agree that the LUMO state is *s*-like, but they disagree substantially as to the dependence of the state energy upon nanocrystal radius. For reference, note that the conduction band state in the bulk has an energy of around 0.4 eV [19].

The disagreement is even more serious for the HOMO. Multiband $\mathbf{k}\cdot\mathbf{p}$ theory not only predicts much lower energies for the HOMO state but also predicts that the HOMO envelope function has odd parity (the state is labelled as $1P_{3/2}$ in the notation of reference [5]). Because of its odd parity, this envelope function has zero overlap with the LUMO envelope function. As a result, multiband $\mathbf{k}\cdot\mathbf{p}$ theory predicts that the fundamental transition to the LUMO occurs from the state below the HOMO (the $1S_{3/2}$ state in the notation of [5]). This contradicts the Wannier function prediction of a simple *s*-like HOMO envelope function. Hence, there is marked disagreement between the theories regarding both the character and the energies of the valence states.

In Fig. 3, the energy of the fundamental transition is presented as a function of nanocrystal radius. The $\mathbf{k}\cdot\mathbf{p}$ fundamental gap is large since it involves a transition from a valence state with such low energy; the gap computed with the Wannier function method is much closer to photoluminescence measurements [16].

The discrepancy between the Wannier function method and the multiband $\mathbf{k}\cdot\mathbf{p}$ method can be understood in the following way. Both the effective mass method and the Wannier function method take the nanocrystal eigenstates to have the form of a slowly varying envelope function times a function with rapid variation within each unit cell, as in equation (6). However, effective mass theory derives a differential equation for the envelope function by assuming that the bulk energy bands $E_n(\mathbf{k})$ may be adequately represented by an expansion to quadratic order in $\mathbf{k}$ [20]. No such

approximation need be made in the Wannier function method and our prediction of the fundamental gap is in much better agreement with experiment as a result. It should be mentioned that, while the multiband $\mathbf{k}\cdot\mathbf{p}$ method makes simplifying assumptions about the form of the bands $E_n(\mathbf{k})$, it does consider the effect of band mixing upon the energy eigenstates. Band mixing is relevant for the Wannier function method since the localization of the functions defined by equation (1) can suffer in the case of degenerate bands. In the presence of degenerate bands, a more complicated multiple band definition of the Wannier functions can improve localization. We find, however, that the Wannier functions defined in the manner of equation (1) are sufficiently well localized for our purposes. As a measure of localization, we determine that the interaction matrix elements (3) between two valence band Wannier functions is small beyond second nearest neighbor lattice points. For two conduction band Wannier functions, the interaction is small beyond fourth nearest neighbors. It is interesting to note that the localization of the valence band Wannier functions is better than the localization of the conduction band Wannier functions even though there are more degenerate bands for valence states than for conduction states.

We now consider transitions beyond the fundamental gap. For InAs, we find that the orbitals in the second highest valence band are nearly degenerate with the orbitals derived from the highest valence band, or $E_v^{\alpha} \approx E_{v2}^{\alpha}$ in the notation of equation (5). Hence, transitions starting from the second highest valence band do not differ substantially in energy from transitions starting in the highest valence band and we do not include them here. To investigate other transitions, we keep in mind the selection rules implied by the dipole matrix element (7).

The highest orbital in the third highest valence band, $f_{v3}^{(1)}$, has an s-like form, similar to that of Fig. 1. Thus, this state is not forbidden from making a transition to the LUMO. The energy of this "s–s" transition is displayed as a function of nanocrystal radius in Fig. 4. The second highest orbital in the highest valence band, $f_v^{(2)}$, has a p-like character, as displayed in Fig. 5. This state therefore cannot make transitions to the s-like LUMO state. However, it can make transitions to the second lowest orbital in the lowest conduction band, $f_c^{(2)}$, which is p-like. The energy of this "p–p" transition is also included in Fig. 4. The predictions displayed in Fig. 4 are in good agreement with preliminary experimental data [21].

In summary, we have predicted InAs nanocrystal electronic transitions using the Wannier function method. Our calculations for the fundamental gap are in good agreement with experimental data, in contrast to the large predictions derived from a recent multiband $\mathbf{k}\cdot\mathbf{p}$ formalism. This success of the Wannier function method is due to our accurate treatment of the bulk energy bands. Predictions of higher electronic transitions are also presented. Further improvements upon the

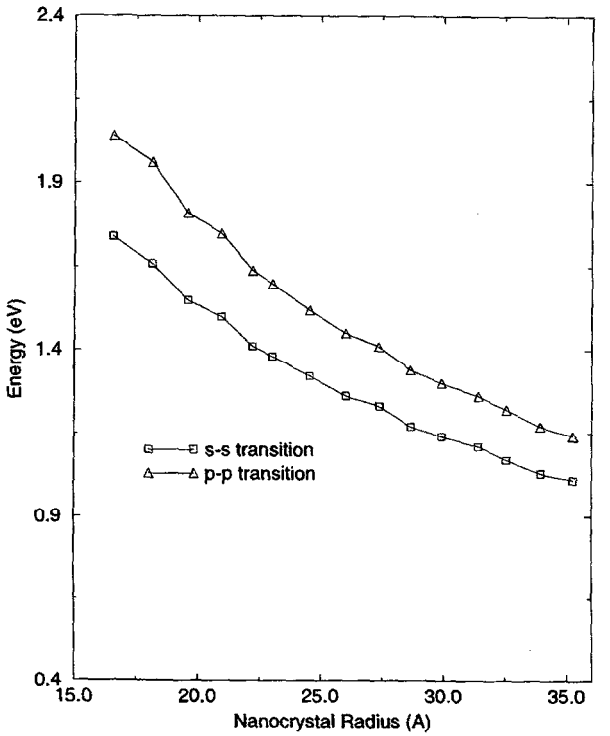

Fig. 4. Transitions with energies larger than fundamental gap.

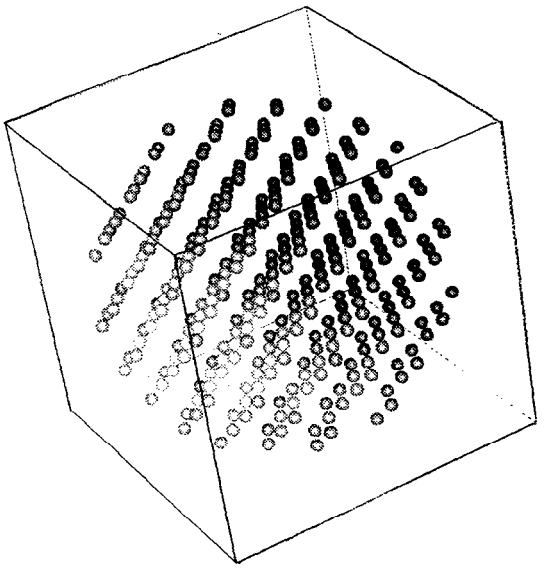

Fig. 5. Second lowest state in the conduction band, $f_c^{(2)}$, has p-like character. Dark spheres have positive $f_c^{(2)}$, light spheres have negative $f_c^{(2)}$.

predictions of the method utilized here could begin with a multiple band definition of the Wannier functions.

Acknowledgements—This work was supported by National Science Foundation grant No. DMR-9520554 and the Director, Office of Energy Research, Office of Basic Energy Services, Materials Sciences Division of the U.S. Department of Energy under Contract No. DE-AC03-76SF00098.

A.M. acknowledges the support of a National Science Foundation Graduate Fellowship.

The authors thank J.R. Chelikowsky, U. Banin and A.P. Alivisatos for helpful discussions.

REFERENCES

1. Alivastos, A.P., *Science*, **271,** 1996, 933.
2. Norris, D.J. and Bawendi, M.G., *Phys. Rev.*, **B53,** 1996, 16338.
3. Vossmeyer, T. *et al.*, *J. Phys. Chem.*, **98,** 1994, 7665.
4. Herron, N., Calabrese, J.C., Farneth, W.E. and Wang, Y., *Science*, **259,** 1993, 1426.
5. Ekimov, A.I., Hache, F., Schanne-Klein, M.C., Ricard, D., Flytzanis, C., Kudryavtsev, I.A., Yazeva, T.V., Rodina, A.V. and Efros, Al.L., *J. Opt. Soc. Am.*, **B10,** 1993, 100.
6. Efros, Al.L. and Efros, A.L., *Sov. Phys. Semicond.*, **16,** 1982, 772.
7. Brus, L.E., *J. Chem. Phys.*, **80,** 1984, 4403.
8. Lippens, P.E. and Lannoo, M., *Phys. Rev.*, **B41,** 1990, 6079; Lippens, P.E. and Lannoo, M., *Phys. Rev.*, **B39,** 1989, 10935.
9. Ramaniah, L.M. and Nair, S.V., *Phys. Rev.*, **B47,** 1993, 7132.
10. Hill, N.A. and Whaley, K.B., *J. Chem. Phys.*, **99,** 1993, 3707.
11. Tomasulo, A. and Ramakrishna, M.V., *J. Chem. Phys.*, **105,** 1996, 3612; Zorman, B., Ramakrishna, M.V. and Friesner, R.A., *J. Phys. Chem.*, **99,** 1995, 7649; Rama Krishna, M.V. and Friesner, R.A., *Phys. Rev. Lett.*, **67,** 1991, 629; Rama Krishna, M.V. and Friesner, R.A., *J. Chem. Phys.*, **95,** 1991, 8309.
12. Wang, L. and Zunger, A., *Phys. Rev.*, **B53,** 1996, 9579; Wang, L., *Phys. Rev.*, **B49,** 1994, 10154; Wang, L. and Zunger, A., *J. Chem. Phys.*, **100,** 1994, 2394; Wang, L. and Zunger, A., *J. Phys. Chem.*, **98,** 1994, 2158.
13. Franceschetti, A. and Zunger, A., *Phys. Rev. Lett.*, **78,** 1997, 915.
14. Mizel, A. and Cohen, M.L., *Phys. Rev.*, **B57,** 1997, 6737.
15. Cohen, M.L. and Chelikowsky, J.R., *Electronic Structure and Optical Properties of Semiconductors*. Springer-Verlag, New York, 1988.
16. Guzelian, A.A., Banin, U., Kadavanich, A.V., Peng, X. and Alivisatos, A.P., *Appl. Phys. Lett.*, **69,** 1996, 1432.
17. Blount, E.I., in *Solid State Physics* (Edited by F. Seitz and D. Turnbull), Vol. 13, p. 305. Academic, New York, 1962.
18. Chelikowsky, J.R. and Cohen, M.L., *Phys. Rev.*, **B14,** 1976, 556.
19. Hermann, C. and Weisbuch, C., in *Optical Orientation* (Edited by F. Meier and B.P. Zakharchenya), p. 467. Elsevier, Amsterdam, 1984.
20. Luttinger, J.M. and Kohn, W., *Phys. Rev.*, **97,** 1955, 869.
21. Banin, U. and Alivisatos, A.P., Personal communication.